ELSEVIER

Biophysical Chemistry 123 (2006) 40–48

Biophysical Chemistry

http://www.elsevier.com/locate/biophyschem

Direct observation of protein folding in nanoenvironments using a molecular ruler

Rupa Sarkar [a], Ajay Kumar Shaw [a], S. Shankara Narayanan [a], Fernando Dias [b], Andy Monkman [b], Samir Kumar Pal [a,*]

[a] *Unit for Nano Science and Technology, S.N. Bose National Centre for Basic Sciences, Block JD, Sector III, Salt Lake, Kolkata 700 098, India*
[b] *Department of Physics, University of Durham, UK*

Received 6 March 2006; received in revised form 6 April 2006; accepted 11 April 2006
Available online 25 April 2006

Abstract

We observe folding of horse heart cytochrome *c* in various environments including nano-compartments (micelles and reverse micelles). Using picosecond-resolved Förster resonance energy transfer (FRET) dynamics of an extrinsic covalently attached probe dansyl (donor) at the surface of the protein to a heme group (acceptor) embedded inside the protein, we measured angstrom-resolved donor–acceptor distances in the environments. The overall structural perturbations of the protein revealed from the FRET experiments are in close agreement with our circular dichroism (CD) and dynamic light scattering (DLS) studies on the protein in a variety of solution conditions. The change of segmental motion of the protein due to imposed restriction in the nano-compartments compared to that in bulk buffer is also revealed by temporal fluorescence anisotropy of the dansyl probe.

Keywords: Cytochrome *c*; Protein folding; Micelles and reverse micelles; Picosecond dynamics; Time-resolved fluorescence anisotropy; Circular dichroism spectroscopy

1. Introduction

Extensive experimental and theoretical efforts are underway to understand how cytochrome *c* (Cytc) folds to its native conformation [1]. Much effort has been focused on spectroscopic techniques including nuclear magnetic resonance [2–4], small angle X-ray scattering [5,6], circular dichroism [7–9], fluorescence [10,11] and Fourier transform infrared spectroscopy [7,12]. Recently, advancement of time-resolved Fourier transform infrared spectroscopy opens a scope for direct observation of protein folding pathways [13,14]. The experiments explore a mechanistic pathway involving a number of intermediates. However, much less experimental efforts have been made to understand the details of a particular intermediate state. Recent studies involving small angle X-ray scattering [5,6] have attempted to distinguish structural changes of the intermediates in the solutions of various denaturant concentrations with respect to that of the native one. Spectroscopic techniques involving Förster resonance energy transfer (FRET) is also one of the possible techniques available, which has the potential to unravel structural details of the intermediates, as the technique is sensitive enough to enable the measurement of inter-residue distance with angstrom (Å) resolution and is known as a 'molecular ruler' [15,16].

In Cytc, the natural choices of FRET donor and acceptor are the single tryptophan (Trp59) and the heme group in the protein, respectively. The fluorescence of the tryptophan (emission peak at 345 nm) in the protein is efficiently quenched (98%) by the soret band of the heme group in Cytc [17]. A number of experimental works [10,17] have already demonstrated the use of Trp59 as a donor in order to study the folding of Cytc. However, the Trp59 may not be a good choice as an energy donor for the following reasons. (I) The soret absorption with large extinction coefficient at 390–410 nm extracts the fluorescence energy of the tryptophan (98%)

* Corresponding author. Fax: +91 33 2335 3477.
E-mail address: skpal@bose.res.in (S.K. Pal).

0301-4622/$ - see front matter © 2006 Elsevier B.V. All rights reserved.
doi:10.1016/j.bpc.2006.04.006

causing negligibly small quantum yield from the Trp59 in the near-native states of the Cytc [17]. The feeble emission from the Trp59 makes spectroscopic detection of the intermediates of Cytc very difficult. (II) The indole group of Trp59 of Cytc is embedded in a very nonpolar environment where ^1L_b state has a dominant role over the ^1L_a state in the absorption of photons, resulting in a de-excitation process through ultrafast internal conversion, $^1L_b \leftrightarrow {}^1L_a$ [18,19]. As the transition dipole moment of ^1L_b and ^1L_a states are mutually orthogonal, the energy transfer from Trp59 to the soret band of the porphyrin ring due to dipole–dipole coupling definitely becomes complex and raise doubts [20,21] in the applicability of simple Förster formulism [22,23] to calculate donor–acceptor distance.

An alternative way of using energy transfer (FRET) experiments is to employ an extrinsic dye as a donor, which should not perturb the native structure of the protein. Recently, FRET experiments on *specifically* dansyl-labeled cytochrome *c* [24] unravel folding landscapes of the protein. However, the potential problem of deciphering global picture of the structural perturbation from a single FRET experiment with specifically labeled protein was unavoidable in the study. In order to gain a overall picture of the unfolded state, the work [24] examined the dansyl-labeled variants of yeast *iso*-1 cytochrome *c* with the fluorophore attached on three different helices (K4C, E66C, K99C) and in three different loops (H39C, D50C, L85C). In contrast to the specific attachment of a donor chromophore at a particular site with respect to acceptor heme group of Cytc, nonspecific labeling at the surface sites distributed all over the protein may become excellent tool for probing global structural perturbation of the protein.

In the present study, we have used the dansyl chromophore (DC) covalently attached to cytochrome *c* (emission maximum 539 nm) as the energy donor. This *non-specific* labeling is well known [25–28], occurs mostly at ε-amino groups of the lysine and arginine residues exposed at the protein surface within the overall structural integrity of the protein. Fluorescence energy of the donor DC is transferred to the Q band absorption of the heme group (absorption maximum 530 nm) [29]. With picosecond-resolved FRET dynamics of DC (donor, D) at the surface of Cytc to the intrinsic heme group (acceptor, A) of native Cytc, we measured two average D–A distances, which are in agreement with high resolution structural NMR and dynamic light scattering (DLS) measurements. The degrees of denaturation of the protein in various denaturant solutions evidenced from the FRET studies are compared with CD and DLS experiments on the protein. We also followed the structural changes of Cytc upon encapsulation in nanometer-sized aqueous pools and upon complexation with various micelles. The structural changes are further confirmed by circular dichroism (CD) studies on the protein in the microenvironments. The time-resolved anisotropy of the donor (DC) in the various nanoenvironments reveals the structural flexibility of the protein. The folding of the denatured protein upon encapsulation in the aqueous pool of AOT reverse micelle is also revealed from our experiments.

2. Materials and methods

Chemicals are obtained from following sources: bis(2-ethylhexyl)sulfosuccinate sodium salt (AOT), TritonX-100 (TX-100), urea, guanidine hydrochloride (GdnCl) from Sigma, bovine pancreatic α-chymotrypsin (CHT) from Sigma, horse heart cytochrome *c* (Cytc) from Aldrich, cetyltrimethylammonium bromide (CTAB) from Fluka, dansyl chloride (DC) from Molecular Probes and isooctane from Romil. The chemicals and the proteins are of highest commercially available purity and used as received. All aqueous solutions are prepared in phosphate buffer. The covalent attachment of DC to Cytc with negligibly small perturbation of the protein structure is achieved following the procedure from Molecular Probes [25] and described in details elsewhere [27,28]. In our labeling, the ratio of DC/Cytc is found to be (1.3):1, considering the soret extinction coefficient of Cytc in buffer at 410 nm as ε_{410}= 106,100 $M^{-1}cm^{-1}$ [2]. DC-labeled cytochrome *c* contains donor (DC) as well as acceptor molecule (heme group). In order to obtain the donor fluorescence lifetime and quantum yield in absence of the acceptor, we have labeled a similar protein, α-chymotrypsin (CHT), with DC. CHT is also a globular protein with diameter (44 Å) similar to that of Cytc (40 Å) and does not contain energy acceptors. The labeling ratio DC/CHT is also found to be (1.5):1. Negligibly small overlap intergral between the absorption and emission spectra of DC molecules [28] rules out intramolecular energy transfer due to multiple labeling of the protein.

The DC-labeled protein-micelle (neutral and cationic) complexes are prepared by mixing measured amount of TX-100 and CTAB respectively with tagged protein (Cytc and CHT) in neutral buffer solutions. In order to impregnate the AOT reverse micelle (RM) with DC-labeled proteins (Cytc and CHT) with various degrees of hydration (w_0), measured volumes of the protein solutions are injected to 2 ml of AOT–isooctane mixture. The degree of hydration (w_0) and radius of water pool (r_0 in Å) of AOT reverse micelle [30] are given by,

$$w_0 = \frac{[\text{Water}]}{\text{AOT}} \tag{1a}$$

$$r_0 = 2 \times w_0 \tag{1b}$$

The solutions of the DC-labeled proteins with GdnCl and urea are kept for 24 h for complete denaturation.

Steady-state absorption and emission are measured with Shimadzu Model UV-2450 spectrophotometer and Jobin Yvon Model Fluoromax-3 fluorimeter respectively. Circular dichroism (CD) is performed with a Spectropolarimeter from Jasco, model J-810 using 0.1 cm path-length quartz cell. Percentage of helical content is computed using the reported computer program [31]. All the experiments are done at room temperature (298±1 K). Picosecond fluorescence transients are obtained by using a home built time correlated single photon counting technique (TCSPC) setup with a diode laser as pump at 385 nm. The emission is detected at magic angle (54.7°) with respect to

the polarization axis of excitation beam using a Hamamatsu MCP photomultiplier tube (2809U). The instrument response function (IRF) for this system is ~60 ps.

In order to study Cytc in bulk buffer, we have used a mode locked Ti Sapphire laser (Coherent, Verdi-V8 pumped picosecond Mira) TCSPC system, using Becker and Hickl acquisition electronics. The second harmonic of the pump laser is tuned at 385 nm. The instrument response function (IRF) for this system is ~23 ps. The observed fluorescence transients are fitted using a nonlinear least squares fitting procedure (software SCIENTIST) to a function comprising of the convolution of the IRF with a sum of exponentials. The purpose of this fitting is to obtain the decays in an analytic form suitable for further data analysis. For anisotropy measurements, emission polarization was adjusted to be parallel or perpendicular to that of the excitation and anisotropy is defined as,

$$r(t) = \frac{[I_{\text{para}} - G \times I_{\text{perp}}]}{[I_{\text{para}} + 2 \times G \times I_{\text{perp}}]} \tag{2}$$

The magnitude of G, the grating factor of the emission monochromator of the TCSPC system, was found by using a coumarin dye in methanol and following longtime tail matching technique [32] to be 1.6.

In order to estimate fluorescence resonance energy transfer efficiency of the donor and hence to determine distances of donor–acceptor pairs, we followed the methodology described in the chapter 13 of Ref. [22] and elsewhere [23]. The Förster distance (R_0) is given by,

$$R_0 = 0.211[\kappa^2 n^{-4} Q_D J(\lambda)]^{1/6} \text{ (in Å)} \tag{3}$$

where κ^2 is a factor describing the relative orientation in space of the transition dipoles of the donor and acceptor. For donor and acceptor that randomize by rotational diffusion prior to energy transfer, the magnitude of κ^2 is assumed to be 2/3. The refractive index (n) of the medium is assumed to be 1.4. The refractive indices of the solutions of 6 M GdnCl and 9 M urea are found to be similar to that of the buffer solution. Q_D, the quantum yield of the donor in the absence of acceptor, is measured from steady-state emission spectrum of DC-labeled CHT in various solutions. $J(\lambda)$, the overlap integral, which expresses the degree of spectral overlap between the donor emission and the acceptor absorption, is given by,

$$J(\lambda) = \frac{\int_0^\infty F_D(\lambda)\varepsilon_A(\lambda)\lambda^4 d\lambda}{\int_0^\infty F_D(\lambda) d\lambda} \tag{4}$$

where $F_D(\lambda)$ is the fluorescence intensity of the donor in the wavelength range of λ to $\lambda + d\lambda$ and is dimensionless. $\varepsilon_A(\lambda)$ is the extinction coefficient (in M^{-1} cm^{-1}) of the acceptor at λ. If λ is in nm, then $J(\lambda)$ is in units of M^{-1} cm^{-1} nm^4.

Once the value of R_0 is known, the donor–acceptor distance (r) can be easily calculated using the formula,

$$r^6 = [R_0^6(1 - E)]/E \tag{5}$$

Here E is the efficiency of energy transfer. The transfer efficiency is measured using the fluorescence lifetimes of the donor, in absence (τ_D) and presence (τ_{DA}) of the acceptor. The efficiency E is also calculated from the following equation:

$$E = 1 - (\tau_{DA}/\tau_D) \tag{6}$$

In order to obtain lifetime of the donor DC at the protein surface in absence of acceptor, we measured the DC-labeled CHT in various solvents including bulk buffer and found two time constants of ~2 ns and 10.5 ns with different preexponential values. As mentioned in the earlier works, the biexponential nature of the fluorescence transient could be due to twisted intra-molecular charge transfer (TICT) process in the DC [26,28,33]. In this study, the faster time constant (~2ns) is regarded as τ_D for τ_{DA} values lower than 2 ns. However, for the τ_{DA} values higher than 2 ns (lower than 10.5 ns), the τ_D is considered to be 10.5 ns.

DLS measurements are done with Nano ZS Malvern instruments employing a 4 mW He–Ne laser (λ=632.8 nm) and equipped with a thermostatted sample chamber. All measurements are taken at 173° scattering angle at 298 K. The scattering intensity data are processed using the instrumental software to obtain the hydrodynamic diameter (d_H) and the size distribution of the scatterer in each sample. The instrument measures the time-dependent fluctuation in intensity of light scattered from the particles in solution at a fixed scattering angle. Hydrodynamic diameters (d_H) of the particles are estimated from the intensity auto correlation function of the time-dependent fluctuation in intensity. d_H is defined as,

$$d_H = kT/3\pi\eta D \tag{7}$$

where k=Boltzmann constant, T=absolute temperature, η=viscosity and D=translational diffusion coefficient. In a typical size distribution graph from the DLS measurement, X-axis shows a distribution of size classes in nm, while the Y-axis shows the relative intensity of the scattered light. This is therefore known as an intensity distribution graph.

3. Results and discussion

Native Cytc in the buffer solution contains a significant amount of α-helix as indicated by absorption in the circular dichroism (CD) spectra at 207 nm and 222 nm [7] (Fig. 1a), which is consistent with high resolution NMR structure of the protein in solution [34]. Upon addition of 9 M urea and 6 M GdnCl, a significant perturbation in the native structure is evident. The numerical fitting parameters of the CD spectra following reported methodology [31] are summarized in Table 1. It is to be noted that the spectral information of Cytc in 9 M urea and 6 M GdnCl solutions below 220 nm are not available because of higher solvent absorption in the spectral range. Significant decrease in CD absorption at 222 nm of Cytc in the denaturant solutions compared to native one clearly indicates insignificant retention of secondary structures in presence of the denaturants. However, in the denaturants, particularly, in the

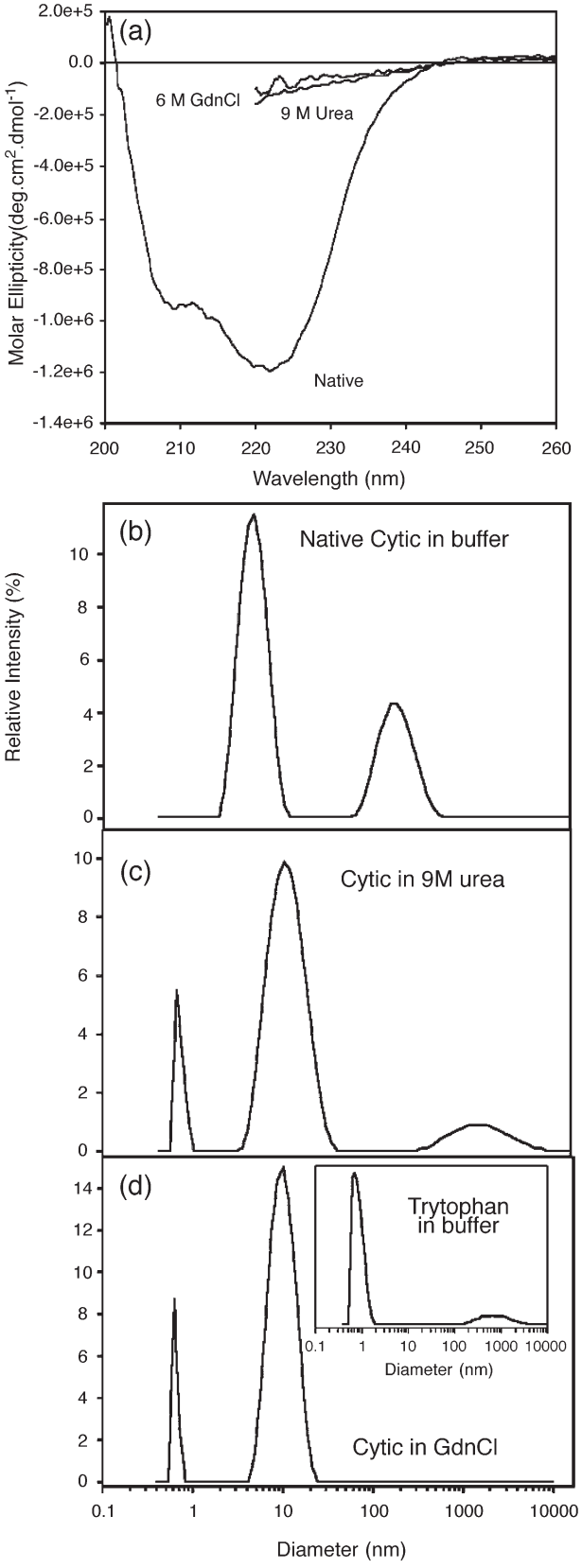

Fig. 1. (a) CD spectra of native (in 50 mM phosphate buffer), 9 M urea and 6 M guanidine chloride (GdnCl) denatured cytochrome *c* in buffer solutions. The numerical fitting of the spectra was done according to literature [31] for the estimation of secondary structures of the protein and summarized in Table 1. Results from dynamic light scattering experiment (DLS) on Cytc in buffer (b), 9 M urea (c), 6 M GdnCl (d) and tryptophan in buffer (inset of panel d) are shown.

Table 1
Numerical fitting parameters of the circular dichroism (CD) spectra of cytochrome c in various environments

Environments	Alpha helix (H)	3/10 Helix (G)	Extended beta strand (E)	Beta turn (T)	Polyproline II like (P)	Others (O)
Cytc in buffer	58%	8%	7%	8%	5%	14%
Cytc in CTAB micelle	40%	6%	15%	11%	7%	21%
Cytc in TX-100 micelle	47%	6%	12%	10%	8%	17%

urea solution the existence of native like topology of the protein can not be completely ruled out [35]. Dynamic light scattering (DLS) studies on the Cytc in buffer solution shows two scattering peaks (Fig. 1b and Table 2). The peak at 4.26 nm is consistent with the hydrodynamic diameter of the monomeric form of Cytc. Note that the estimated diameter from the solution NMR structure of the protein is 3.6 nm [34]. Considering the thickness of the hydration layer to be ~0.4 nm [27], our observation of the hydrodynamic diameter is in good agreement with the structural NMR study.

The structural perturbation in urea and GdnCl solutions are evidenced in Fig. 1c and d, respectively. The numerical values of the hydrodynamic diameters in the denaturant solutions are summarized in Table 2. In the denaturant solutions, the main peaks show hydrodynamic diameter to be 10 nm indicating swelling of the protein structure upon denaturation. One of the possible reasons of the peaks at 0.6 nm in the solutions is due to hydrolysis of some of the amino acids of the protein. The conjecture is further supported by DLS measurement of hydrodynamic diameter of an amino acid tryptophan in the buffer solution as shown in the inset of Fig. 1d (data in Table 2). The experiment clearly shows a major peak at 0.8 nm, indicating typical hydrodynamic diameter of an amino acid. The peaks due to particles with higher hydrodynamic diameter (100 nm and larger) could be due to the presence of aggregation of the solutes in the solutions. Note that in the intensity distribution graph the area of the peak for the larger particles will appear at least 10^6 times larger than the peak for the smaller particles. This is because large particles scatter much more light than small particles, as the intensity of scattering of a particle is proportional to the sixth power of its diameter (Rayleigh's

Table 2
Dynamic light scattering (DLS) data for the hydrodynamic diameters of Cytc in various solutions are summarized

Solutions	Scattering peaks	Hydrodynamic diameter (nm)	Relative intensity (%)	Width (nm)
Cytc in buffer	Peak 1	4.26	67.7	1.35
	Peak 2	148	32.3	60.7
Cytc in 9 M urea	Peak 1	0.681	10.1	0.075
	Peak 2	10.1	78.9	4.49
	Peak 3	1310	11.0	902
Cytc in 6 M GdnCl	Peak 1	0.644	11.4	0.042
	Peak 2	10.4	88.6	3.30
Tryptophan in buffer	Peak 1	0.829	86.9	0.198
	Peak 2	1050	13.1	782

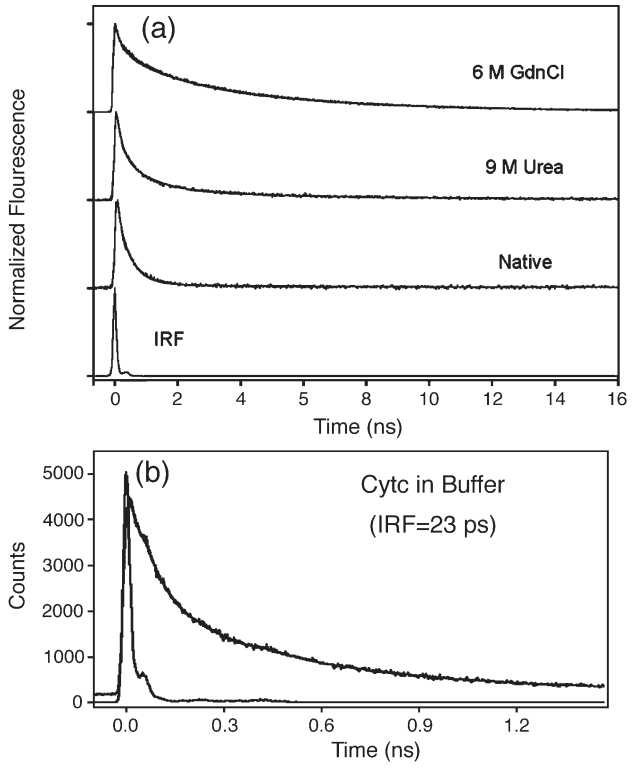

Fig. 2. (a) Picosecond-resolved fluorescence transients of DC-labeled cytochrome *c* in various solutions. (b) Time-resolved fluorescence transient of DC-labeled cytochrome *c* in buffer (IRF = 23 ps).

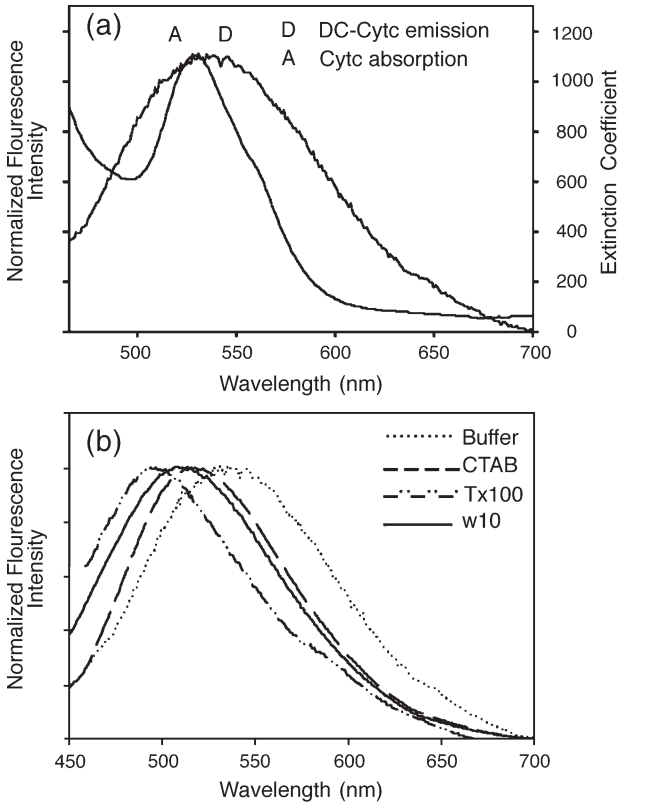

Fig. 3. (a) Spectral overlap between the donor (dansyl-Cytc) emission and acceptor (heme group of Cytc) absorption is shown. (b) Fluorescence spectra of DC-labeled cytochrome *c* in various microenvironments.

approximation). Thus the number densities of larger particles in our solutions are negligibly small.

The structural perturbations of the protein in buffer and denaturant solutions are also clearly evident by picosecond-resolved fluorescence transients (Fig. 2a). The numerical fittings of the transients are summarized in Table 3. As seen from Table 3, the fluorescence transient of DC-labeled Cytc shows significant faster component (90 ps (23.3%)), which is close to the IRF of the instrument (60 ps). In order to resolve faster time constants, we have studied the sample using a Mira pumped TCSPC system (Fig. 2b, IRF 23 ps). Three decay components with time constants 24.7 ps (51%), 132.4 ps (32%) and 640 ps (17%) are obtained in the time window of 1.5 ns. The faster decay components of the native form compared to those of Cytc with various degrees of denaturation (in urea and GdnCl solutions) indicate efficient FRET of the dansyl chromophore to the heme group of the protein in the former case.

Table 3
Numerical fitting parameters of the fluorescence transients of DC-labeled cytochrome *c* in various solutions

Solutions	τ_1 (ns)	τ_2 (ns)	τ_3 (ns)
Cytc in buffer	0.09 (23.3%)	0.44 (73.8%)	10.5 (2.9%)
Cytc in 9 M urea solution	0.20 (53.8%)	1.1 (39.2%)	9.3 (7.0%)
Cytc in 6 M GdnCl solution	0.19 (3.7%)	1.9 (25.4%)	5.7 (70.9%)
Cytc in CTAB micelle	0.42 (2.3%)	3.8 (51.7%)	10.9 (46%)
Cytc in TX-100 micelle	0.15 (46.3%)	1.1 (47.8%)	10.5 (5.9%)
Cytc in RM (w_0 = 10)	0.40 (29.3%)	1.9 (43.3%)	10.5 (27.4%)
Cytc in RM (w_0 = 20)	0.65 (25.6%)	2.7 (30.2%)	10.5 (44.3%)
Cytc in 9 M urea solution in RM (w_0 = 10)	0.34 (25.5%)	1.9 (46.4%)	8.1 (28.1%)

The spectral overlap of the donor (DC-labeled Cytc; emission maximum at 539 nm) emission and unlabeled Cytc (Q band of heme group; absorption maximum at 530 nm) absorption as shown in Fig. 3a, is one of reasons for the efficient FRET [22]. The D–A distances obtained from FRET experiments are summarized in Table 4. The average donor acceptor distances in Cytc in buffer (11.99 Å and 16.10 Å) are in agreement with the shortest and longest distances of the acceptor (heme group) from the protein surface (11.51 Å and 24.52 Å) as estimated from solution NMR structure of Cytc [34]. The degree of unfolding in the urea and GdnCl solutions is clearly evident from Tables 2–4. Time-resolved emission spectra of Cytc in 6 M GdnCl shows much higher percentage of unfolded species (70%) compared to that in 9 M urea solution (7%), indicating efficacy of the former solution as potential denaturant of the protein. As summarized in Table 4 in the Cytc, the maximum D–A distance in the GdnCl solution (31.5 Å) is also larger than that in the urea solution (26.8 Å).

In order to gain the nature of the folding of Cytc in various microenvironments, we have studied D–A distances in micelles and reverse micelles with various degrees of hydration (w_0). Fig. 3b shows steady-state emission spectra of dansyl-labeled Cytc in various microenvironments. A significantly large solvatochromic shift of the DC at the surface of Cytc in various nanoenvironments is clearly evident. The blue shift of the DC-

Table 4
Energy transfer parameters of cytochrome *c* in different environments

System	Overlap integral (M^{-1} cm^{-1} nm^4)	R_0 (Å)	Q_D	τ_{DA}	τ_D	τ_{DA}/τ_D	r (Å)
Cytc in buffer	4.78×10^{13}	20.33	0.097	0.09	2.2	0.040	11.99
				0.44		0.198	16.10
				10.5	10.5	–	–
Cytc in 9 M urea solution	4.68×10^{13}	19.05	0.067	0.20	2.099	0.095	13.08
				1.1		0.524	19.36
				9.3	10.5	0.886	26.8
Cytc in 6 M GdnCl solution	6.08×10^{13}	20.50	0.08	0.19	2.1	0.087	13.98
				1.9		0.887	31.50
				5.7	10.5	0.543	21.09
Cytc in CTAB micelle	5.19×10^{13}	26.62	0.45	0.42	2.2	0.191	20.92
				3.8	10.5	0.363	24.23
				10.5		–	–
Cytc in TX-100 micelle	4.97×10^{13}	21.86	0.144	0.15	2.2	0.070	14.20
				1.1		0.497	21.82
				10.5	10.5	–	–
Cytc in RM (w_0=10)	4.08×10^{13}	18.93	0.0742	0.40	1.8	0.222	15.36
				1.9	10.5	–	–
				10.5		–	–
Cytc in RM (w_0=20)	5.78×10^{13}	20.07	0.0641	0.65	1.57	0.414	18.60
				2.7	10.5	0.259	16.85
				10.5		–	–
Cytc in 9 M urea solution in RM (w_0=10)	1.66×10^{14}	18.07	0.00589	0.34	2.7	0.124	11.33
				1.9		0.700	18.07
				8.1	10.5	0.771	19.22

R_0, Q_D, τ_D, τ_{DA} and r denote Förster distance, quantum yield of the donor and donor lifetime in absence of acceptor, donor lifetime in presence of acceptor and estimated donor–acceptor distance, respectively.

Cytc-micelle complexes compared to the DC-Cytc in bulk buffer clearly indicates that a significant portion of Cytc surface is involved in the complexation with the micelles. The emission maximum of DC-Cytc in the RM (511 nm at w_0=10) does not depend upon the degree of hydration (w_0) of the RM. The observation is consistent with the fact that Cytc resides at the interface of the RM [36] and the viscosity/polarity of immediate environment of the protein hardly depends on the size (radius of the aqueous pool) of the RM. Even when denatured protein is incorporated inside the reverse micelle of w_0=10, no significant change in emission maximum is observed.

As evidenced from Fig. 4a (CD absorption at 222 nm), the α-helical structures of the protein upon complexation with TX-100 and CTAB micelles are not altered significantly compared to that in buffer. This type of small perturbation of protein structure of CHT upon complexation with CTAB micelles is also evidenced in a recent study [37]. Note that spectral information below 210 nm is unavailable due to huge background absorption from the host micellar solutions. The picosecond-resolved fluorescence transients (Fig. 4b) of dansyl-labeled Cytc in buffer and in different micellar (neutral (TX-100) and cationic (CTAB)) environments are fitted to sum of exponentials convoluted with the instrument response function (IRF). The fitting results are summarized in Table 3. As evidenced from Table 4, donor acceptor distances in Cytc upon complexation with the micelles are significantly different from that in native protein, indicating binding interactions of the micelles with Cytc affects compaction of the protein. The geometrical restriction on the DC at the Cytc surface upon complexation with CTAB micelle is evidenced from the time-resolved fluorescence anisotropy (Fig. 4c). The anisotropy transient decays exponentially almost to the baseline with time constants 110 ps (48.8%) and 4.7 ns (51.2%); the anisotropy at t=0 (r_0) is 0.39 (Table 5). Previous studies [10] of time-resolved fluorescence anisotropy on the intrinsic tryptophan (Trp59) of apocytochome *c* in various viscous buffer solutions shows three distinct time constants of ~150 ps, ~1.0 ns and 5.0 ns. In the study [10], faster depolarization components (150 ps and 1 ns) and slower 5 ns component were assigned as local tumbling motion of Trp59 and average rotation of the overall protein, respectively. Our observation of time-resolved anisotropy of covalently attached DC reflecting physical motions of the probe are in agreement with the previous study [10].

The protein Cytc is insoluble in isooctane and extremely soluble in water. Thus upon injection of the protein into the AOT reverse micellar solution Cytc is expected to reside in the RM. The incorporation is also evidenced from the blue solvatochromic shift in the steady-state emission spectrum (Fig. 3b). Small angle X-ray scattering experiments confirm that Cytc resides at the isooctane–water interface of the RM [36]. Recent NMR [3] study shows that upon incorporation of the protein inside anionic (AOT) reverse micelle, a significant structural perturbation compared to that in free buffer due to charge interaction between the protein and the surfactant, which is consistent with our CD studies (data not shown). The fluorescence transients of dansyl-labeled Cytc in RM with various degrees of hydrations are shown in Fig. 5a and the numerical fittings are summarized in Table 3. Estimated donor–

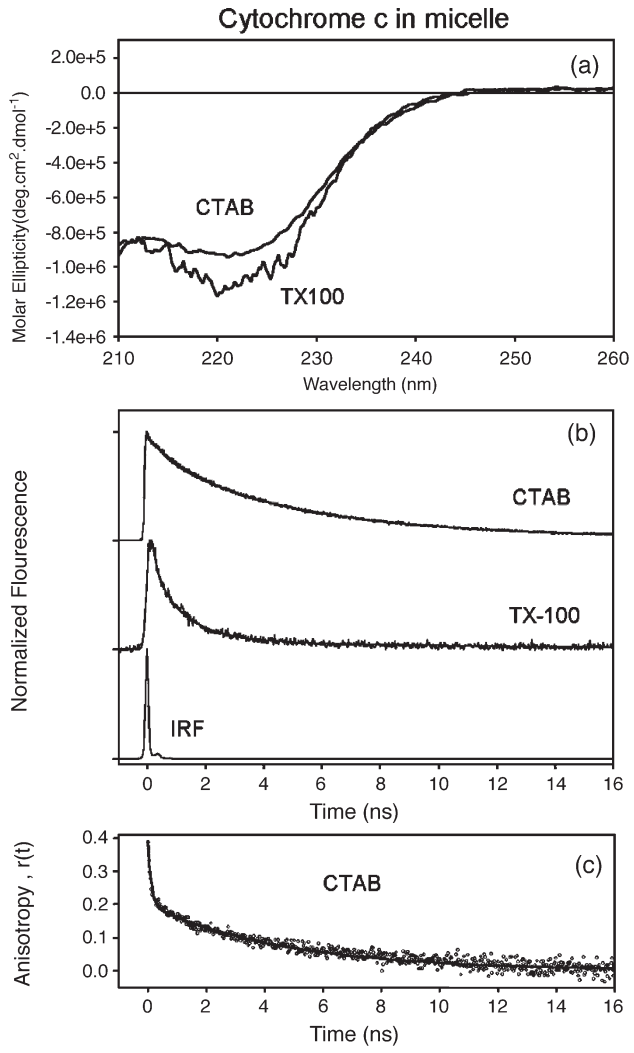

Fig. 4. (a) CD spectra of cytochrome *c* in 5 mM CTAB and 1.68 mM TX-100 micelle in 50 mM phosphate buffer at 27 °C. 0.1 cm path-length quartz cell used. (b) Picosecond-resolved fluorescence transients of DC-labeled cytochrome *c* in buffer, TX-100 and CTAB micelle. (c) Time-resolved fluorescence anisotropy, *r* (*t*) of DC-Cytc in CTAB micellar environment.

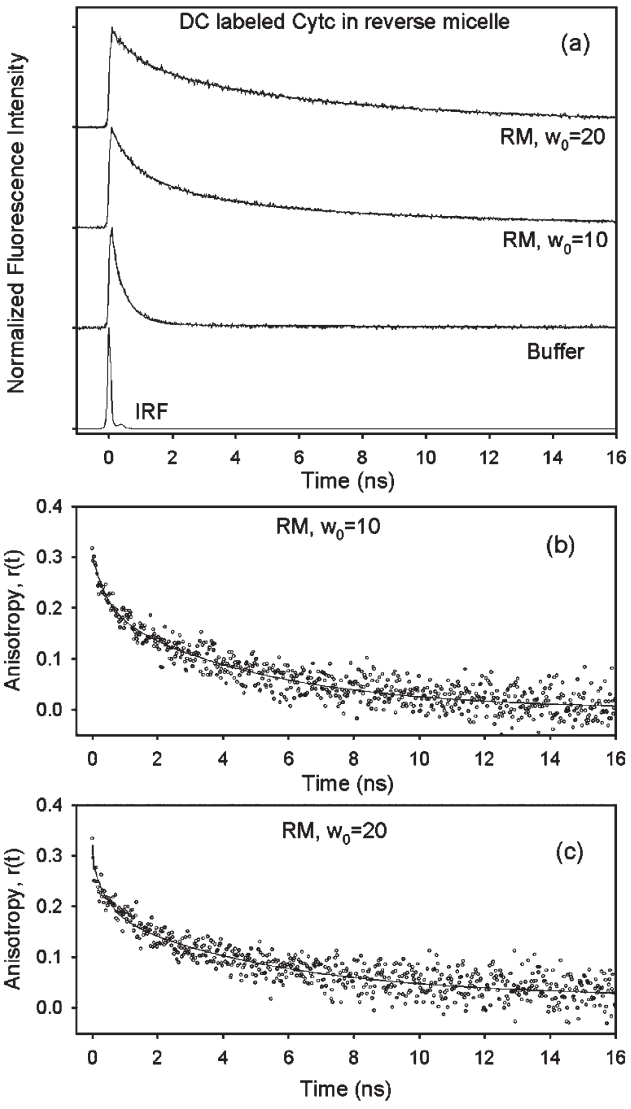

Fig. 5. (a) Picosecond-resolved fluorescence transients of DC labeled Cytc in RM at $w_0=10$ and $w_0=20$. Transient of DC-Cytc in buffer is also shown for comparison. (b) Time-resolved fluorescence anisotropy of the DC-labeled protein inside RM ($w_0=10$). (c) Picosecond-resolved fluorescence anisotropy of DC-Cytc in the RM ($w_0=20$).

acceptor distances are given in Table 4. In contrast to the Cytc in bulk buffer, the amplitudes of the fast components (400 ps at $w_0=10$ and 650 ps at $w_0=20$), which depicts that the average population of donor DC responsible for energy transfer process, decreases upon incorporation of the protein in the RM. The observation may be suggestive of significant structural perturbation in the anionic RM due to strong charge interaction.

Table 5
Numerical fitting parameters of time-resolved fluorescence anisotropy of DC-labeled cytochrome *c* in various environments

Systems	τ_1 (ns)	τ_2 (ns)	τ_3 (ns)	r_0
Cyto in CTAB micelle	0.11 (48.8%)	4.7 (51.2%)	–	0.39
Cyto in RM ($w_0=10$)	0.45 (33.1%)	4.8 (66.9%)	–	0.32
Cyto in RM ($w_0=20$)	0.44 (32.8%)	5.0 (56.3%)	50 (10.9%)	0.28
Denatured Cyto in RM ($w_0=10$)	0.10 (75%)	2.8 (25%)	–	0.40

The time-resolved anisotropy studies (Table 5) show local environmental rigidity of the probe dansyl of the DC-Cytc complex incorporated in the RM with various degrees of hydration. Fig. 5b and c show the anisotropy of Cytc in RM at $w_0=10$ and $w_0=20$, respectively. The initial anisotropy, r_0, for both the cases starts from ~0.3 and ends to almost zero within 16 ns time window (time constants, 450 ps (33.1%), 4.8 ns (66.9%) at $w_0=10$ and 440 ps (32.75%), 5.0 ns (56.3%) and 50 ns (10.9%) at $w_0=20$). The fast component with time constant ~450 ps in the reverse micelles is slower than the bulk buffer indicating the local tumbling motion of DC is restricted in the nanocage of RM. The component of 4.8 ns indicates the segmental motion of the DC-labeled protein. The 50 ns component found in the RM at $w_0=20$ could be the characteristics for the global motion of the Cytc included in the larger nanocage. The absence of 50 ns temporal decay of *r*(*t*)

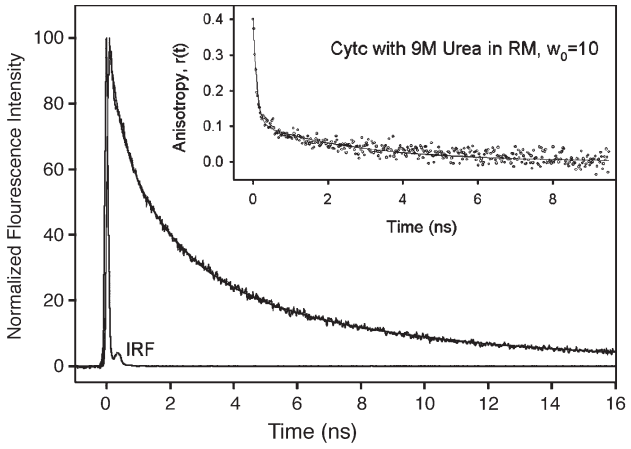

Fig. 6. Picosecond-resolved fluorescence transients of denatured DC-Cytc in buffer and in the RM (w_0=10). Inset shows temporal fluorescence anisotropy of denatured DC-Cytc in the RM (w_0=10).

of Cytc in RM of w_0=10 can be due to insufficient reporter DC molecules (Table 3) with longer lifetime (10.5 ns).

In a recent work refolding of denatured Cytc upon encapsulation of the protein in AOT-RM has been reported [38]. The study demonstrated that unfolded Cytc following denaturation by 9 M urea resembles compact folded structure in the AOT-RM. Here we have studied the nature of folding of the urea-denatured Cytc in the RM. Fig. 6 shows fluorescence transient of 9 M urea denatured protein in the RM, w_0=10. The numerical fitting parameters and estimated D–A distances are summarized in Tables 3 and 4, respectively. As evidenced from Table 4, the donor–acceptor distances (11.29 Å and 17.99 Å) of the protein in the RM with urea are comparable to the average distance in the RM without urea (15.34 Å). This observation does not indicate any dramatic refolding of the denatured Cytc in the nanoenvironment of the RM.

However, a significant structural perturbation of Cytc in the RM with urea compared to that in the RM without urea is evident from temporal fluorescence anisotropy of DC-Cytc in the respective media (inset of Figs. 5b and 6, Table 5). In the RM (w_0=10), anisotropy of the denatured protein starts at 0.4 (r_0) and goes almost to zero within 10 ns time window. $r(t)$ decays bi-exponentially with time constants 100 ps (75%) and 2.8 ns (25%) as shown in the inset of Fig. 6. The existence of the heavily weighted fast dynamics in the anisotropy decay clearly indicates labile state of the protein in the RM compared to that in the RM without urea (Fig. 5b). An attempt has been made to study the renaturation of GdnCl denatured Cytc upon encapsulation in the RM. However, the protein solution with 6M GdnCl is found to be insoluble in RM.

4. Conclusion

Studies of Förster resonance energy transfer (FRET) of a dansyl probe covalently bound at the surface of cytochrome *c* to the heme group of the protein in various environments including nanometer-sized reverse micellar aqueous cage show the nature of folding in the environments and the effect of degree of hydration (size) of the RM on the folding compaction. Circular dichroism (CD) and dynamic light scattering (DLS) experiments on the folding pattern of Cytc in the microenvironments are in good agreement with the FRET studies on the protein. The nonradiative energy transfer method employed in this work can be effectively used in characterizing the structure and dynamics of folding of other heme proteins.

Acknowledgement

RS and AKS would like to thank UGC; SSN would like to thank CSIR for their fellowships. We acknowledge financial support from the Durham University Photonic Materials Institute and CENAMS (ONE NorthEast).

References

[1] R.A. Goldbeck, Y.G. Thomas, E. Chen, R.M. Esquerra, D.S. Kliger, Multiple pathways on a protein-folding energy landscape: kinetic evidence, Proc. Natl. Acad. Sci. U. S. A. 96 (1999) 2782–2787.
[2] B.S. Russell, R. Melenkivitz, K.L. Bren, NMR investigation of ferricytochrome *c* unfolding: detection of an equilibrium unfolding intermediate and residual structure in the denatured state, Proc. Natl. Acad. Sci. U. S. A. 97 (2000) 8312–8317.
[3] B.G. Lefebvre, W. Liu, R.W. Peterson, K.G. Valentine, A.J. Wand, NMR spectroscopy of proteins encapsulated in a positively charged surfactant, J. Magn. Reson. 175 (2005) 158–162.
[4] R.W. Peterson, K. Anbalagan, C. Tommos, A.J. Wand, Forced folding and structural analysis of metastable proteins, J. Am. Chem. Soc. 126 (2004) 9498–9499.
[5] S. Akiyama, T. Kimura, K. Ishimori, I. Morishima, Conformational landscape of cytochrome *c* folding studied by microsecond-resolved small angle X-ray scattering, Proc. Natl. Acad. Sci. U. S. A. 99 (2002) 1329–1334.
[6] M. Flanagan, M. Kataoka, D. Shortle, Truncated staphylococcal nuclease is compact but disordered, Proc. Natl. Acad. Sci. U. S. A. 89 (1992) 748–752.
[7] Q. Xu, T.A. Keiderling, Effect of sodium dodecyl sulfate on folding and thermal stability of acid denatured cytochrome *c*: a spectroscopic approach, Protein Sci. 13 (2004) 2949–2959.
[8] K. Naoe, K. Noda, M. Kawagoe, M. Imai, Higher order structure of proteins solubilized in AOT reverse micelle, Colloids Surf., B Biointerfaces 38 (2004) 179–185.
[9] G.A. Elove, A.F. Chaffotte, H. Roder, M.E. Goldberg, Early steps in cytochrome *c* folding probed by time-resolved circular dichroism and fluorescence spectroscopy, Biochemistry 31 (1992) 6876–6883.
[10] M. Vincent, J.-C. Bronchon, F. Merola, W. Jordi, J. Gallay, Nanosecond dynamics of horse heart apocytochrome *c* in aqueous solution as studied by time-resolved fluorescence of the single tryptophan residue (Trp-59), Biochemistry 27 (1988) 8752–8761.
[11] M.C.R. Shastry, M.R. Eftink, Reversible thermal unfolding of ribonuclease T1 in reverse micelles, Biochemistry 35 (1996) 4094–4101.
[12] A. Dong, T. Lam, Equilibrium titrations of acid induced unfolding-refolding and salt-induced molten globule of cytochrome *c* by FT-IR spectroscopy, Arch. Biochem. Biophys. 436 (2005) 154–160.
[13] C. Kotting, K. Gerwert, Time-resolved FTIR studies provide activation free energy, activation enthalpy and activation entropy for GTPase reactions, Chem. Phys. Lett. 307 (2004) 227–232.
[14] C. Kotting, K. Gerwert, Proteins in action monitored by time-resolved FTIR spectroscopy, ChemPhysChem 6 (2005) 881–888.
[15] A.K. Shaw, R. Sarkar, S.K. Pal, Direct observation of DNA condensation in a nano-cage by using a molecular ruler, Chem. Phys. Lett. 408 (2005) 366–370.

[16] C.S. Yun, A. Javier, T. Jennings, M. Fisher, S. Hira, S. Peterson, B. Hopkins, N.O. Reich, G.F. Strouse, Nanometal surface energy transfer in optical rulers, breaking the FRET barrier, J. Am. Chem. Soc. 127 (2005) 3115–3119.
[17] T.Y. Tsong, Ferricytochrome *c* chain folding measured by the energy transfer of tryptophan 59 to the heme group, Biochemistry 15 (1976) 5467–5473.
[18] X.H. Shen, J. Knutson, Subpicosecond fluorescence spectra of tryptophan in water, J. Phys. Chem., B 105 (2001) 6260–6265.
[19] S.K. Pal, A.H. Zewail, Dynamics of water in biological recognition, Chem. Rev. 104 (2004) 2099–2123.
[20] R.E. Dale, J. Eisinger, W.E. Blumberg, The orientational freedom of molecular probes. The orientation factor in intramolecular energy transfer, Biophys. J. 26 (1979) 161–193.
[21] R.E. Dale, J. Eisinger, Intramolecular distances determined by energy transfer. Dependence of orientational freedom of donor and acceptor, Biopolymers 13 (1974) 1573–1605.
[22] J.R. Lakowicz, Principles of Fluorescence Spectroscopy, Kluwer Academic/Plenum, New York, 1999.
[23] P. Majumder, R. Sarkar, A.K. Shaw, A. Chakraborty, S.K. Pal, Ultrafast dynamics in a nanocage of enzymes: solvation and fluorescence resonance energy transfer in reverse micelles, J. Colloid Interface Sci. 290 (2005) 462–474.
[24] E.V. Pletneva, H.B. Gray, J.R. Winkler, Many faces of the unfolded state: conformational heterogeneity in denatured yeast cytochrome *c*, J. Mol. Biol. 345 (2005) 855–867.
[25] R.P. Haugland, Handbook of Fluorescent Probes and Research Chemicals, Molecular Probes, Eugene, OR, 1996.
[26] D. Zhong, S.K. Pal, A.H. Zewail, Femtosecond studies of protein-DNA binding and dynamics: histone I, ChemPhysChem 2 (2001) 219–227.
[27] S.K. Pal, J. Peon, A.H. Zewail, Biological water at the protein surface: dynamical solvation probed directly with femtosecond resolution, Proc. Natl. Acad. Sci. U. S. A. 99 (2002) 1763–1768.
[28] R. Sarkar, M. Ghosh, A.K. Shaw, S.K. Pal, Ultrafast surface solvation dynamics and functionality of an enzyme chymotrypsin upon interfacial binding to a cationic micelle, J. Photochem. Photobiol., B Biol. 79 (2005) 67–78.
[29] A.A. Andrade, N.M. Barbosa Neto, L. Misoguti, L. De Boni, S.C. Zilio, C. R. Mendonca, Two-photon absorption investigation in reduced and oxidized cytochrome *c* solutions, Chem. Phys. Lett. 390 (2004) 506–510.
[30] R. Biswas, S.K. Pal, Caging enzyme function: α-chymotrypsin in reverse micelle, Chem. Phys. Lett. 387 (2004) 221–226.
[31] W.C. Johnson, Analyzing protein circular dichorism spectra for accurate secondary structures, Proteins Struct. Funct. Genet. 35 (1999) 307–312.
[32] D.V. O'Connor, D. Philips, Time Correlated Single Photon Counting, Academic Press, London, 1984.
[33] R. Sarkar, M. Ghosh, S.K. Pal, Ultrafast relaxation dynamics of a biologically relevant probe dansyl at the micellar surface, J. Photochem. Photobiol., B Biol. 78 (2005) 93–98.
[34] L. Banci, I. Bertini, H.B. Gray, C. Luchinat, T. Reddig, A. Rosato, P. Turano, Solution structure of oxidized horse heart cytochrome *C*, NMR, minimized average structure, Biochemistry 36 (1997) 9867–9877.
[35] D. Shortle, M.S. Ackerman, Persistance of native like topology in a denatured protein in 8 M urea, Science 293 (2001) 487–489.
[36] M.P. Pileni, T. Zemb, C. Petit, Solubilization by reverse micelles: solute localization and structure perturbation, Chem. Phys. Lett. 118 (1985) 414–420.
[37] M.S. Celej, M.G. D'Adrea, P.T. Campana, G.D. Fidelio, M.L. Bianconi, Superactivity and conformational changes on α-chymotrypsin upon interfacial binding to cationic micelles, Biochem. J. 378 (2004) 1059–1066.
[38] M. Sakono, M. Goto, S. Furusaki, Refolding of cytochrome *c* using reversed micelles, J. Biosci. Bioeng. 89 (2000) 458–462.